Optical spectra of free and supported CuCl microcrystals produced by thermal evaporation in a helium gas stream

1994 J. Phys.: Condens. Matter 6 1269

(http://iopscience.iop.org/0953-8984/6/6/029)

J. Phys.: Condens. Matter 6 (1994) 1269–1278. Printed in the UK

Optical spectra of free and supported CuCl microcrystals produced by thermal evaporation in a helium gas stream

Shōsuke Mochizuki†, Hitoshi Nakata† and Raphael Ruppin‡

† Department of Physics, College of Humanities and Sciences, Nihon University, 3-25-40 Sakurajosui, Setagaya-ku, Tokyo 156, Japan

‡ Department of Applied Physics and Mathematics, Soreq Nuclear Research Centre, Yavne 70600, Israel

Received 18 May 1993, in final form 29 September 1993

Abstract. Time-resolved measurements of the extinction spectra of free CuCl microcrystals and of CuCl microcrystals collected on a glass substrate have been performed at various growth stages after the beginning of evaporation in a low-pressure helium gas. Absorption bands due to $Z_{1,2}$ and Z_3 excitons were observed, which were shifted in energy from their bulk positions owing to exciton confinement effects. Initially the energy difference between the $Z_{1,2}$ and the Z_3 bands is considerably larger than its bulk value, and with increasing time it decreases and approaches the bulk value. The observed Z_3 exciton absorption bands are compared with those calculated using an extended Mie theory, in which non-local effects as well as the size quantization of the excitonic states are included.

1. Introduction

Optical properties of semiconductor microcrystals have received much attention recently, providing information on the three-dimensional confinement of electrons, holes and excitons [1]. Such microcrystals also have potential applications as materials having large optical non-linearities [2, 3]. Theoretically, with decreasing crystal size, the quantization of exciton motion, arising from the confining potential, has to be taken into account. When the particle size decreases further and approaches the exciton Bohr radius, the character of the exciton disappears and the electrons and holes become individually confined [1]. Until now, most of the microcrystals used in such studies were embedded in a transparent matrix or were capped with other molecules. Thus, for small crystallites, the effects caused by the surroundings (e.g. induced shape distortion and energy transfer) may have interfered with the exciton confinement effects in which we are interested. Therefore, it is desired to study the optical properties of free microcrystals as a function of crystal size without embedding or capping. For this purpose, it is best to produce a size (mass)-selected microcrystal beam with a high number density in free space and then to measure various optical properties in the temperature region for stable excitons. However, at present, the number density of size-selected microcrystals available is too low for the usual optical measurements. Recently, we have developed a simple measurement method using the time-resolved and space-resolved spectroscopies of the vapour zone produced by thermal evaporation in helium gas and have already applied it to the study of metal clusters and microcrystals [4–7]. Very recently, we have also applied it to the study of several semiconductors, CuCl, CuBr, CuI, CdS and ZnS.

In the present paper, we report, for the first time, the time-resolved optical extinction spectra of a CuCl vapour zone produced by thermal evaporation in a low-pressure helium gas

0953-8984/94/061269+10$07.50

stream. CuCl is a suitable material for the study of confinement effects on exciton motion for the following reasons. CuCl is a direct-transition-type semiconductor and the valence band is split into two bands by the spin–orbit interaction, which yields two kinds of exciton, namely $Z_{1,2}$ and Z_3. Also, the exciton binding energies are larger than 200 meV, which guarantees the observation of excitonic absorption up to high temperatures. Moreover, the exciton Bohr radius has the very small value of 0.68 nm, which enables us to study exciton confinement effects even in very small crystallites. Using CuCl microcrystals grown in glass [8–10] or alkali chloride crystals [11-13], several interesting optical properties due to exciton confinement have been reported.

2. Experimental details

Experiments were carried out using the apparatus described previously [4–7]. An alumina crucible containing nominally pure CuCl powder was electrically heated by a tungsten-wire heater which was wound around the crucible and the surface was coated with alumina. Experiments on free CuCl microcrystals were carried out as follows. The temperature of the crucible was gradually increased by applying a constant voltage. Prior to the optical measurements, the temperatures of representative positions in the vapour zone were measured with a thermocouple under the same conditions of gas evaporation as those in which the optical measurements would be made. The optical spectra of selected positions in the vapour zone were recorded in a transmission configuration as a function of time elapsed after the beginning of the evaporation. Continuum light from a 150 W Xe lamp was directed at the whole vapour zone above the crucible through an optical window without using a lens. After passing through the vapour zone, only the light through a selected position was collected with a lens and then spectrally analysed and recorded with an optical multichannel analyser system.

Experiments on supported CuCl microcrystals were carried out by introducing a liquid-nitrogen tank into the gas evaporation chamber described above. A silica glass substrate was attached to the bottom of the tank and was cooled. The temperature of the substrate was measured with a thermocouple. The substrate was at a height of 112 mm above the crucible edge. After the beginning of evaporation, transmissivity spectra were measured as a function of time using the same optical analyser system as for free microcrystals. For free and supported microcrystals, the transmissivity is the intensity ratio of the transmitted radiation during the evaporation through the vapour zone and the substrate, respectively, to that before the evaporation.

Since the transmissivity spectra T_r contain the effects of both scattering and absorption, the results are expressed as extinction spectra $-\log T_r$.

3. Results

3.1. Free CuCl microcrystals

Figure 1(*a*) shows the time-resolved spectrum obtained at the vapour zone at a height of 3 mm above the crucible edge. The gas evaporation was carried out in a helium gas stream at a pressure of 1.5 Torr and a flow rate of 0.5 l min^{-1}. Although one time-resolved spectrum consists of 32 spectra, at time intervals of 2 s, in this figure, only the spectra from the eighteenth spectrum are presented in order to show clearly the time evolution. The measured temperatures of the vapour zone are 406 K, 445 K and 472 K for the first,

seventeenth and thirty-second spectra, respectively. At the initial stage of the evaporation, a broad band appears at about 368 nm. The band is accompanied by a shoulder on its longer-wavelength side. With progressing gas evaporation, the band becomes sharper and, together with its shoulder, shifts to longer wavelengths. The observed band and shoulder are due to the $Z_{1,2}$ and Z_3 exciton absorptions, respectively, in CuCl. In order to show the exciton absorption in detail, figure 1(*b*) is given. The energies are blue-shifted considerably from their bulk values. On further progressing gas evaporation, the band and shoulder continue to shift, with a growing long-wavelength tail. Also, the extinction at wavelengths shorter than 350 nm increases, with a band growing at about 270 nm and shifting to longer wavelengths with progressive gas evaporation.

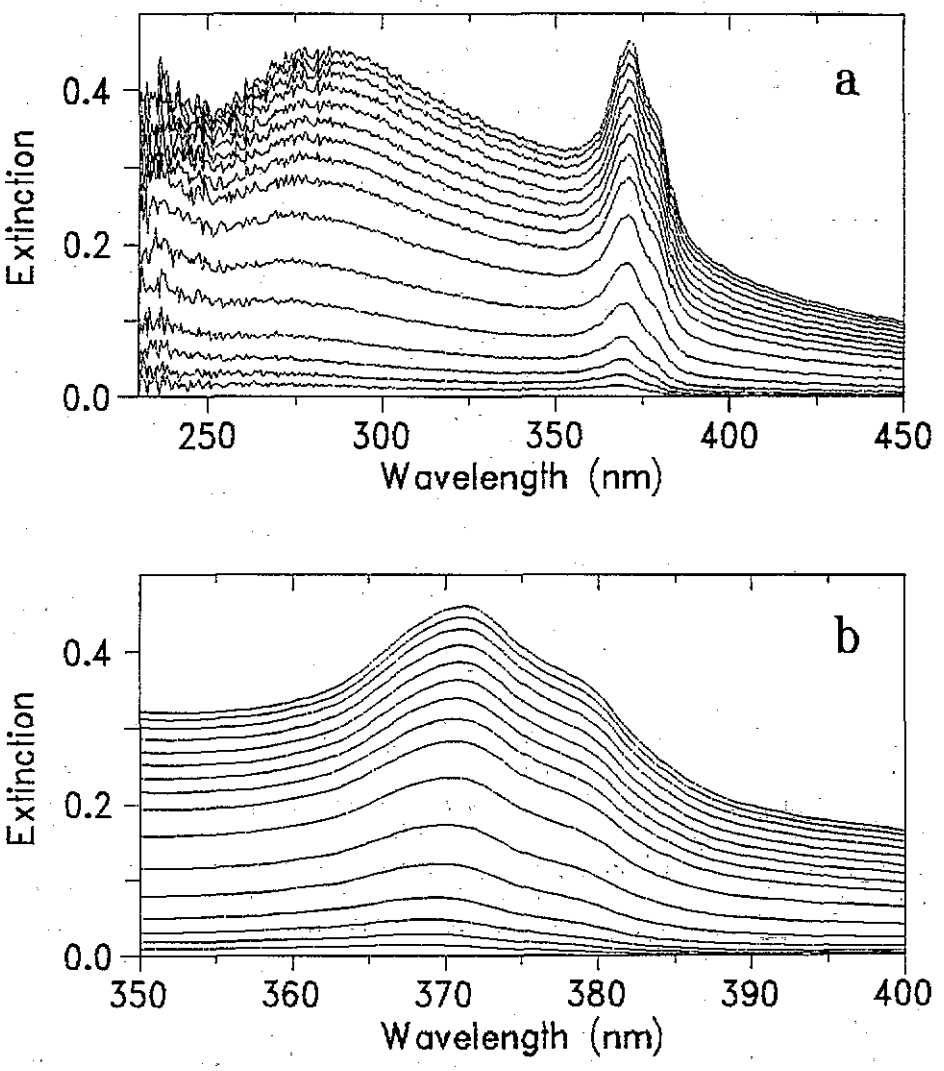

Figure 1. Time-resolved extinction spectra of free CuCl microcrystals.

Figures 2(*a*) and 2(*b*) show the time dependence of the energies of the extinction peak and shoulder due to the $Z_{1,2}$ and Z_3 exciton absorptions, respectively. The peak energy ($Z_{1,2}$

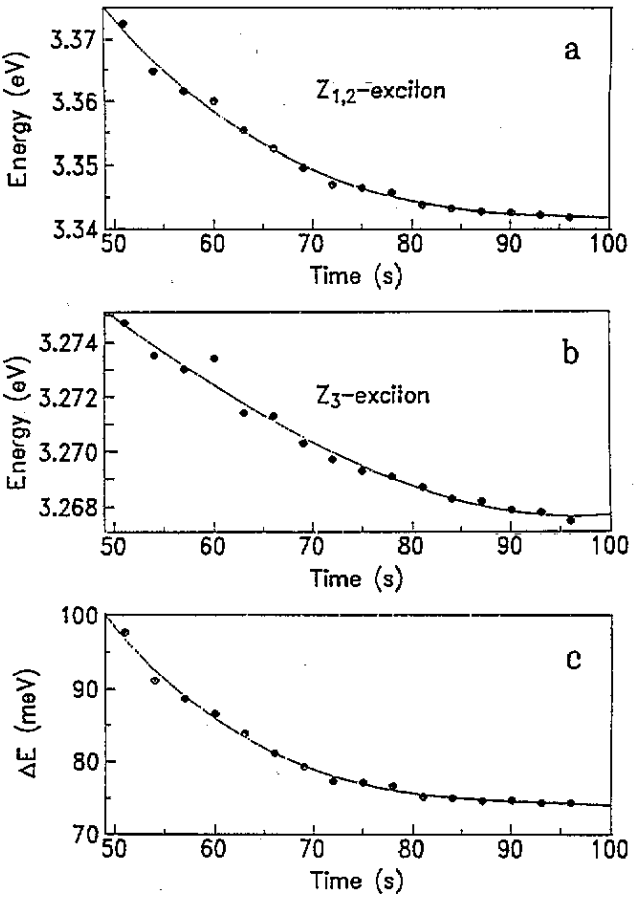

Figure 2. Time dependence of exciton energies of free CuCl microcrystals: (*a*) energy of the $Z_{1,2}$ exciton; (*b*) energy of the Z_3 exciton; (*c*) energy difference between the $Z_{1,2}$ and Z_3 excitons.

exciton) was determined by finding the wavelength at which the first derivative with respect to the wavelength was zero, while the shoulder energy (Z_3 exciton) was determined by finding the wavelength at which the second derivative with respect to the wavelength was a maximum. Also, the energy difference E between the peak and shoulder energies is shown in figure 2(*c*). Approaching the steady state of gas evaporation, the energy difference tends smoothly to the observed energy difference (about 70 meV) between $Z_{1,2}$ and Z_3 excitons in bulk CuCl [14]. This indicates that the observed time evolution arises from exciton confinement in the CuCl microcrystals.

3.2. CuCl microcrystals supported on silica substrate

Figure 3 shows the time-resolved extinction spectra during gas evaporation. The condition for gas evaporation was the same as that for free microcrystals. The temperature of the silica substrate was kept at 93 K. Since the extinction of the substrate coated with microcrystals is determined by the thickness of the accumulated microcrystal layer, the change in the extinction is faster than that in the vapour zone. Therefore, the time interval between two

successive spectra was set to 990 ms. As shown in figure 3, the $Z_{1,2}$ and Z_3 bands are better resolved than those of free microcrystals; this is due to a fall in the temperature of the microcrystals. The peak energies are shifted considerably from their bulk values towards high energies. With progressive gas evaporation, these bands shift to longer wavelengths and their widths decrease. Also, a band at wavelengths shorter than 300 nm and a tail on the long-wavelength side of the Z_3 band are observed, as in the case of free microcrystals. The time dependences of the $Z_{1,2}$ exciton energy, the Z_3 exciton energy and their energy difference ΔE are shown in figures 4(*a*), 4(*b*) and 4(*c*), respectively. Since the *n*th spectrum also contains the contribution of the accumulated microcrystal layer, which was already measured as the $(n-1)$th spectrum, we determined the peak energies of *n*th spectrum after subtracting the $(n-1)$th spectrum from the *n*th spectrum. As in the case of free microcrystals, with progressive gas evaporation, the energy difference of the supported microcrystals smoothly approaches the bulk value of about 70 meV. This indicates that the observed time evolution arises from exciton confinement in the CuCl microcrystals. Optically, we could not find any temperature difference between the microcrystals and the substrate. This is probably because the helium gas remains around the substrate and the microcrystals have a small heat capacity.

3.3. Miscellaneous

3.3.1. Gas evaporation of $CuCl_2$. It is often mentioned that CuCl easily oxidizes and transforms to $CuCl_2$. On the other hand, it is known that $CuCl_2$ decomposes to produce CuCl at high temperatures. To rule out the possibility that the observed spectra were affected by oxidation, we have thermally evaporated $CuCl_2$ under the same conditions as those applied to CuCl. Some of the observed time-resolved spectra are shown in figure 5. Spectra 1, 2 and 3 were measured at 128 s, 131 s and 158 s, respectively, after the beginning of evaporation. At the initial stage of gas evaporation, the spectrum is very broad and completely different from that of CuCl described above. However, with progressive gas evaporation, the absorptions due to $Z_{1,2}$ and Z_3 excitons grow to produce a band similar to that shown in figure 1(*a*). This indicates that $CuCl_2$ is unstable to heating in a low-pressure helium gas stream and transforms to CuCl.

3.3.2. Air exposure effect on CuCl microcrystals. After measurement of the spectra at low temperatures, the CuCl microcrystals supported on a silica substrate were naturally warmed to room temperature in vacuum and then were exposed slowly to air. The time-resolved extinction spectra measured during the exposure showed that, with increasing exposure time, the spectrum broadens gradually and the exciton structure disappears. This indicates that CuCl microcrystals may absorb water vapour in air and then transform into a mixture consisting of CuCl, $CuCl_2$ and other complex salts. However, x-ray diffraction for the specimen just after exposure to air shows a sharp and intense line due to (111) reflection on the CuCl lattice. No lines due to $CuCl_2$ or other salts were observed, which indicates that the main component of the mixture is CuCl.

4. Discussion

4.1. Estimate of the average size of the microcrystals

As shown in sections 3.1 and 3.2, the time evolution of the optical spectrum of CuCl microcrystals is similar for the two types of specimen (free and supported specimens). We

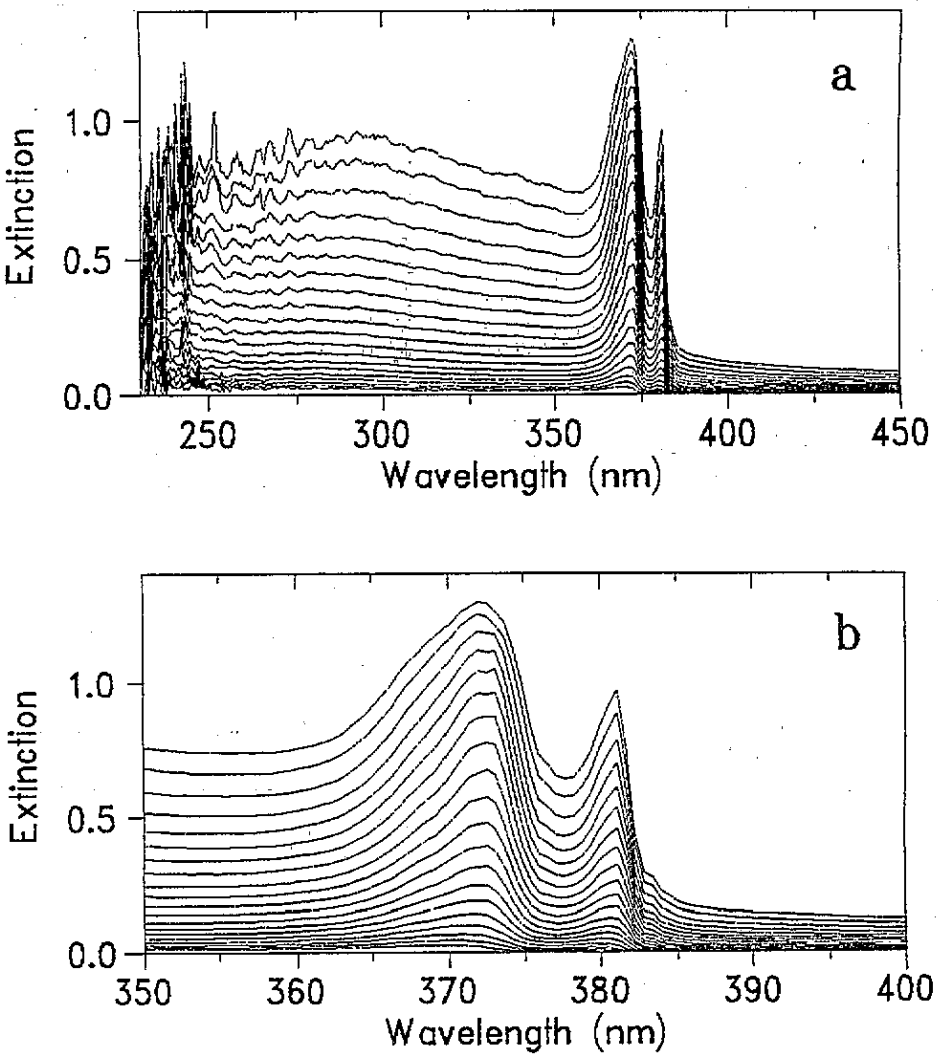

Figure 3. Time-resolved extinction spectra of CuCl microcrystals supported on silica.

cannot determine directly the size of the microcrystals, because of the chemical instability of CuCl in air.

However, it is possible to estimate the sizes by comparing the observed exciton peaks with those calculated from an extended version of the Mie theory, in which non-local effects and the size quantization of the exciton motion are taken into account [15]. It should be noted that the exciton transition energies increase with increasing temperature while, in spite of the temperature increase during evaporation, the observed peaks shift to lower energies with progressive evaporation. This indicates that shifts due to exciton confinement are indeed involved.

The generalized Mie theory [15] enables us to calculate the extinction cross section of spherical microcrystals in the vicinity of an excitonic transition of frequency ω_T, where the dielectric constant, which is both frequency and wavenumber dependent, can be written in the form

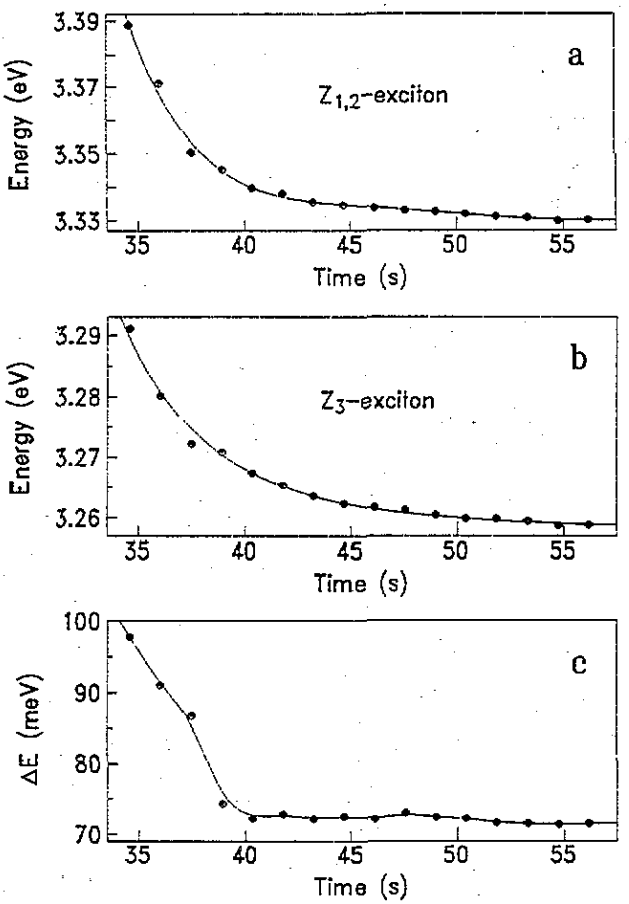

Figure 4. Time dependence of exciton energies of CuCl microcrystals supported on silica: (*a*) energy of the $Z_{1,2}$ exciton; (*b*) energy of the Z_3 exciton; (*c*) energy difference between the $Z_{1,2}$ and Z_3 excitons.

$$\epsilon(\omega, k) = \epsilon_0 + \omega_p^2/(\omega_T^2 - \omega^2 + Dk^2 - i\gamma\omega) \tag{1}$$

where ϵ_0 is the background dielectric constant, ω_p is a measure of the oscillator strength, γ is the damping constant and $D = \hbar\omega_T/M$, where M is the exciton mass. The appropriate values of these parameters for the Z_3 exciton of CuCl were taken from the experimental data in [11, 12]. However, since the latter data were obtained at lower temperatures than those employed in our experiments, we have to take into account the increase in the bulk transition energy of the Z_3 exciton with increasing temperature. We have estimated this increase by using the experimental data of Masumoto *et al* [13]. They have presented absorption spectra of a given sample of CuCl microcrystals of mean radius 6.1 nm at various temperatures in the range 20–250 K. Using the extended Mie theory [15], we have calculated the position of the Z_3 absorption peak for such crystallites. We have found that the calculated peak energy agrees with the experimental value if the temperature dependence of the bulk exciton energy is estimated from

$$E(Z_3) = 3.2103 + 2.17 \times 10^{-4}T - 9.5 \times 10^{-8}T^2(\text{eV}). \tag{2}$$

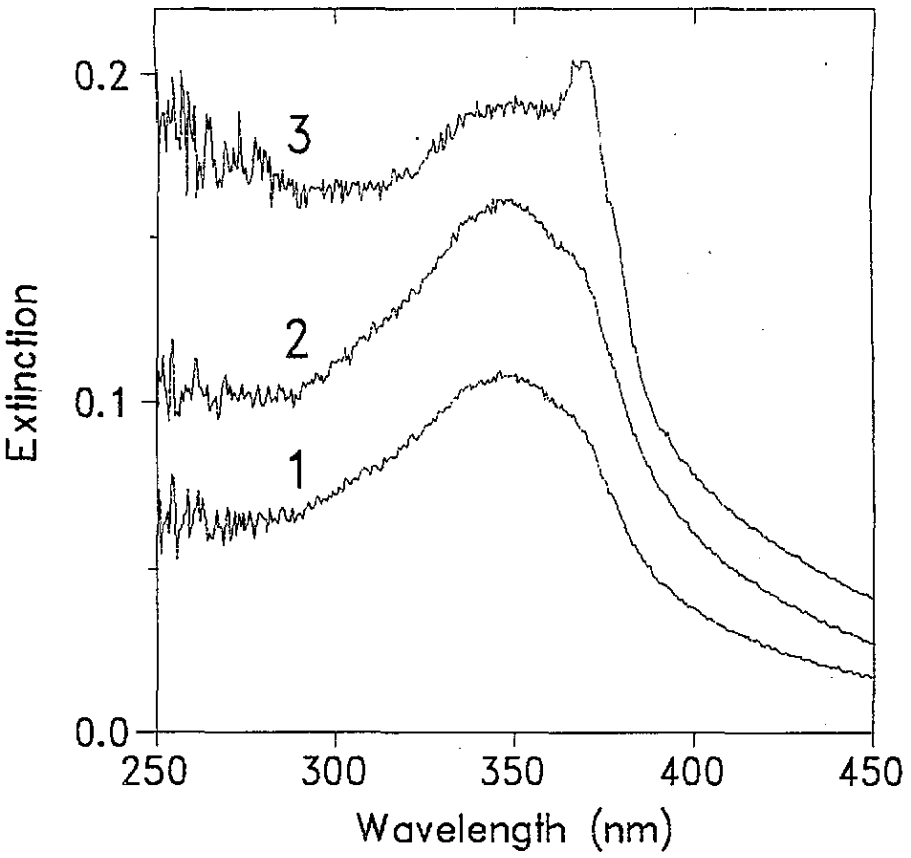

Figure 5. Extinction spectra of the vapours from the crucible containing $CuCl_2$ obtained 128 s (spectrum 1), 131 s (spectrum 2) and 158 s (spectrum 3) after beginning the evaporation.

Next, the extinction spectra were calculated for spherical crystallites at 93 K, which is the substrate temperature. We note that electron micrograph images taken by Hayashi and Yamamoto [16] have shown that CuCl microcrystals produced by gas evaporation are indeed spherical in shape. The calculations were performed for various sizes, in an attempt to find out which sizes yield Z_3 peaks in the experimental range 378–381 nm. The effects of size distribution, which usually exist, were taken into account in the calculation. A normal distribution of sizes was assumed, with an average diameter d, and a standard deviation of $\frac{1}{5}d$ around this value. The extinction spectra calculated for average sizes of 2.8 nm, 3.1 nm, 3.4 nm and 3.9 nm are shown in figure 6. These sizes yield extinction peaks at 378 nm, 379 nm, 380 nm and 381 nm, respectively, and the peak width decreases with increasing size, as observed experimentally (figure 3). The blue shift of the exciton peak with decreasing crystalline size is a well known effect arising from the confinement of the exciton motion [1]. On the basis of these calculations of the Z_3 peak it is estimated that the microcrystals supported on silica (figure 3) had a size of about 2.8 nm in the first stages, increasing later to about 3.9 nm.

The sizes of the free microcrystals (figure 1) cannot be estimated by this method, because the Z_3 peak appears only as a shoulder of the $Z_{1,2}$ peak. Also, an analogous calculation of the $Z_{1,2}$ peak is not possible because no simple representation of the dielectric constant of

the form (1) exists in the vicinity of the $Z_{1,2}$ exciton frequency.

4.2. Energy difference between $Z_{1,2}$ and Z_3 excitons

The energy difference between and the intensity ratio of the $Z_{1,2}$ and Z_3 absorptions in CuCl depend on the strengths of the spin–orbit and exchange interactions. Although it is very difficult to calculate exactly the size dependence of the energy difference, we performed the following simple estimate. For a microcrystal of radius a, the confined exciton energies can be approximated from the dispersion relation $E(k)$, evaluated at $k = \pi/a$. For the calculations, we have used the dispersion relations in the ⟨111⟩ direction quoted by Itoh *et al* [11]. The Z_3 exciton dispersion is given by their equation (3). For the $Z_{1,2}$ exciton, there occurs a splitting into three energies when $k = 0$, given by their equations (1) and (2). We assumed that the centre of the observed $Z_{1,2}$ band is simply the average of these three energies. From the graphs given by Itoh *et al*, we estimated that the bulk energy difference is 71 meV. Using the parameters given in their table 1 and only the dispersion in the ⟨111⟩ direction, we obtained the size dependence of the energy difference $\Delta E = E(Z_{1,2}) - E(Z_3)$ at 77 K, as shown in figure 7. The calculated size trend seems to explain qualitatively our experimental results shown in figures 2(*c*) and 4(*c*). This may indicate that the strengths of the spin–orbit and exchange interactions of free and supported microcrystals are almost the same as for bulk CuCl.

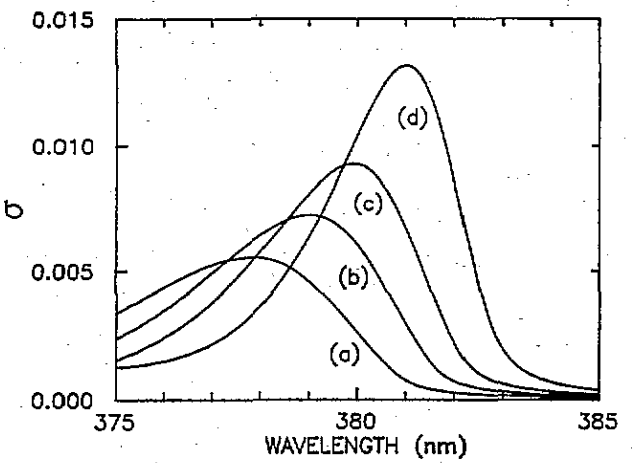

Figure 6. Calculated extinction spectra of CuCl spheres for various average sphere diameters ⟨*d*⟩: spectrum (*a*), 2.8 nm; spectrum (*b*), 3.1 nm; spectrum (*c*), 3.4 nm; spectrum (*d*), 3.9 nm.

4.3. Other comments

Since an exact calculation of the extinction is possible only when the frequency- and wavevector-dependent complex dielectric constant is known, we cannot compare the spectra obtained in present study with theoretical spectra in the entire experimental spectral region, except for the Z_3 exciton band. Therefore, at present, the origin of the observed extinction band at wavelengths shorter than 350 nm is not clear.

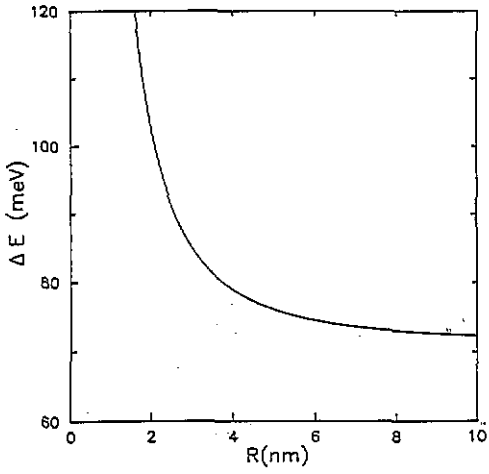

Figure 7. Calculated energy difference between $Z_{1,2}$ and Z_3 excitons at 77 K.

Acknowledgments

This study was supported in part by a Grant-in-Aid for Scientific Research from the Ministry of Education (Japan). This study was also supported in part by a Grant-in-Aid (1991, 1993) for Overseas Research from Nihon University. The authors would like to thank Professor Tadashi Itoh (Tohoku University) for several useful discussions and several communications of some unpublished data. The authors also acknowledge Mr Teruya Kusuda for assistance with the measurements.

References

[1] Efros Al L and Efros A L 1982 *Fiz. Tekh. Poluprov.* **16** 1209 (Engl. Tran. 1982 *Sov. Phys.–Semicond.* B **16** 772)
[2] Hanamura E 1988 *Phys. Rev.* B **37** 1237
[3] Itoh T 1991 *Nonlinear Opt.* **1** 61
[4] Mochizuki S 1991 *Phys. Lett.* **155A** 510
[5] Mochizuki S 1992 *Phys. Lett.* **164A** 191
[6] Mochizuki S and Ruppin R 1993 *J. Phys.: Condens. Matter* **5** 135
[7] Mochizuki S 1993 *Phys. Lett.* **176A** 382
[8] Ekimov A I, Efros Al L and Onushchenko A A 1985 *Solid State Commun.* **56** 921
[9] Ekimov A I, Onushchenko A A, Raikh M E and Efros Al L 1986 *Zh. Eksp. Theor. Fiz.* **90** 1795 (Engl. transl. 1986 *Sov. Phys.–JETP* **63** 1054)
[10] Nakamura A, Yamada H and Tokizaki T 1989 *Phys. Rev.* B **40** 8585
[11] Itoh T, Iwabuchi Y and Kirihara T 1988 *Phys. Status Solidi* b **146** 531
[12] Itoh T, Iwabuchi Y and Kataoka M 1988 *Phys. Status Solidi* b **145** 567
[13] Masumoto Y, Wamura T and Iwaki A 1989 *Appl. Phys. Lett.* **55** 2535
[14] Kato Y, Goto T, Fujii T and Ueta M 1974 *J. Phys. Soc. Japan* **36** 169
[15] Ruppin R 1989 *J. Phys. Chem. Solids* **50** 877
[16] Hayashi S and Yamamoto K 1987 *J. Phys. Soc. Japan* **56** 2229
[17] Itoh T and Furumiya M 1991 *J. Lumin.* **48–9** 704